Cluster Compounds

Linear, Redox-Active Pt_6 and $Pt_2Pd_2Pt_2$ Clusters**

Eri Goto, Rowshan A. Begum, Shuzhong Zhan, Tomoaki Tanase, Katsumi Tanigaki, and Ken Sakai*

Transition metal clusters, which contain multinuclear metal sites connected by metal–metal bonds in a variety of geometrical structures, have attracted increasing attention due to their versatile chemical and physical properties as well as their potential to integrate multiple functions in a single molecule.[1] In particular, clusters that show linear metal–metal bonding have been regarded as promising candidates in developing nanostructured materials including molecular electronic, optical, and chemical devices. However, synthetic methods using self-assembly of metal atoms often lead to polyhedral cluster cores, and thus routes to molecules with linear metal aggregations are limited.[2–7] We have studied homo- and heterometallic dinuclear and trinuclear complexes supported by the tridentate phosphane ligand bis(diphenylphosphanylmethyl)phenylphosphane (dpmp).[8] The linearly ordered trinuclear complexes $[Pt_2M(\mu\text{-dpmp})_2(XylNC)_2](PF_6)_2$ (M = Pt (**1a**), Pd (**1b**); Xyl = 2,6-dimethylphenyl) were prepared by site-selective incorporation of a zero-valent Pt or Pd atom into the diplatinum complex $[Pt_2(\mu\text{-dpmp})_2(XylNC)_2](PF_6)_2$.[8c] In the present study, we have examined a cluster core expansion of **1**, and have successfully synthesized linear hexametallic clusters containing a redox-active $Pt_2M_2Pt_2$ metal string (M = Pt, Pd).

When the linear triplatinum complex **1a** was treated with excess $NaBH_4$ in ethanol, and the resultant brown precipitate was extracted and stirred in CH_2Cl_2, the dark blue, diamagnetic hexaplatinum cluster $[Pt_6(\mu\text{-H})(\mu\text{-dpmp})_4(XylNC)_2](PF_6)_3$ (**2**) was isolated in good yield (Scheme 1).

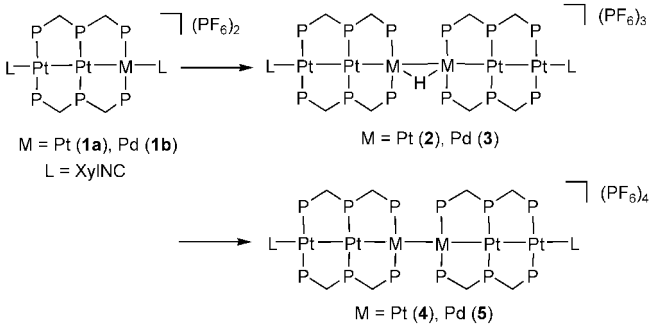

Scheme 1. Synthesis of **2**–**4**. $\widehat{PPP}$ = dpmp

Compound **2** was also obtained in low yield from the reaction of **1** with NaOMe. Although the Pt_2Pd trinuclear complex **1b** failed to be expanded with $NaBH_4$, it readily reacted with NaOMe in CH_2Cl_2/MeOH to afford dark green crystals of $[Pt_4Pd_2(\mu\text{-H})(\mu\text{-dpmp})_4(XylNC)_2](PF_6)_3$ (**3**, Scheme 1). The changes in the ESI mass spectrum and the electronic absorption spectrum during the reaction to form **2** indicated that the initial brown compound, assigned as $[Pt_3(H)_2(\mu\text{-dpmp})_2(XylNC)]^{2+}$ (**A**), was rapidly converted into $[Pt_3(H)(\mu\text{-dpmp})_2(XylNC)]^{+}$ (**B**) in CH_2Cl_2. It is assumed that the monohydride intermediate **B** undergoes coupling and concomitant partial oxidation to generate complex **2**. However, the intervening species were not identified.[9]

The crystal structure of **2** was determined by X-ray analysis.[10] The cluster cation of **2** has a charge of +3 with a cluster valence electron count (CVE) of 86. It consists of six linearly ordered platinum atoms (Pt-Pt-Pt 174.87(2)–179.67(2)°) bridged by four dpmp ligands and terminated by two isocyanide molecules (Figure 1). The Pt_6 cluster core has a pseudo C_2 symmetry, and the average Pt–Pt distances are 2.7041 Å for the outer Pt1–Pt2 and Pt5–Pt6 bonds (d_{out}), 2.7329 Å for the inner Pt2–Pt3 and Pt4–Pt5 bonds (d_{inn}), and 3.3092(5) Å for the central Pt3–Pt4 bond (d_{cen}). The values for d_{out} and d_{inn} are comparable to those of the triplatinum complex **1**[8] and indicate the presence of Pt–Pt σ bonds. Although the two central platinum atoms are not supported by any organic ligands and are sterically well protected by the four phenyl groups of the dpmp ligands, the remarkably long distance d_{cen} indicates the presence of a bridging hydride; this was unambiguously confirmed by ^1H NMR spectroscopy.

[*] Dr. E. Goto, Dr. R. A. Begum, Dr. S. Zhan, Prof. Dr. T. Tanase
Department of Chemistry
Faculty of Science
Nara Women's University
Kitauoya-higashi-machi, Nara 630-8285 (Japan)
Fax: (+81) 742-20-3399
E-mail: tanase@cc.nara-wu.ac.jp
Prof. Dr. K. Tanigaki
Department of Physics
Graduate School of Science
Tohoku University
Aoba-ku, Sendai 980-8578 and CREST, JST (Japan)
Prof. Dr. K. Sakai
Department of Applied Chemistry
Faculty of Science
Tokyo University of Science
Kagurazaka 1-3, Shinjuku-ku, Tokyo 162-8601 (Japan)

[**] This work was partly supported by Grants-in-Aid for Scientific Research from the Ministry of Education, Culture, Sports, Science and Technology, Japan.

Supporting information for this article is available on the WWW under http://www.angewandte.org or from the author.

 DOI: 10.1002/ange.200460707

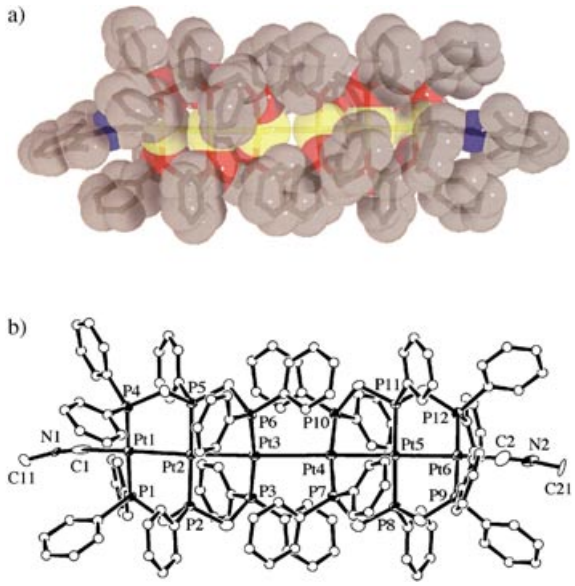

Figure 1. Crystal structure of **2**. a) A perspective plot with van der Waals radii superimposed on a wire-frame view; Pt yellow, P red, N blue, C gray. b) An ORTEP plot showing the linearly aligned coordinatively unsaturated metal sites; the xylyl rings have been omitted for clarity. Selected bond distances [Å] and angles [°]: Pt1–Pt2 2.7073(5), Pt2–Pt3 2.7333(5), Pt3–Pt4 3.3092(5), Pt4–Pt5 2.7325(5), Pt5–Pt6 2.7008(5), Pt1–P1 2.300(3), Pt1–P4 2.299(3), Pt2–P2 2.254(2), Pt2–P5 2.255(2), Pt3–P3 2.268(3), Pt3–P6 2.264(3), Pt4–P7 2.266(2), Pt4–P10 2.269(2), Pt5–P8 2.248(2), Pt5–P11 2.256(2), Pt6–P9 2.291(2), Pt6–P12 2.303(2), Pt1–C1 2.02(1), Pt6–C2 1.94(1), N1–C1 1.12(1), N2–C2 1.19(1); Pt1-Pt2-Pt3 174.87(2), Pt2-Pt3-Pt4 178.47(2), Pt3-Pt4-Pt5 179.40(2), Pt4-Pt5-Pt6 179.67(2), Pt2-Pt1-C1 177.1(3), Pt5-Pt6-C2 177.0(3), Pt1-C1-N1 172.6(8), Pt6-C2-N2 176.3(9).

According to the X-ray crystal structure,[11] the cluster cation of **3** is isomorphous to **2** (see the Supporting Information). It contains a $Pt_2Pd_2Pt_2$ hexametallic chain (M-M-M 175.10(2)-179.71(3)°) in which the central two metal positions are site-selectively occupied by Pd atoms and bridged by a hydride. The metal–metal distances are slightly longer than the corresponding values for **2** ($d_{out} = 2.7184$ Å (Pt–Pt), $d_{inn} = 2.7498$ Å (Pt–Pd), $d_{cen} = 3.355(1)$ Å (Pd–Pd)).

The ^{1}H NMR spectrum of **2** exhibited the resonance for the bridging hydride at $\delta = -8.6$ ppm, accompanied by a set of ^{195}Pt satellite peaks from two chemically equivalent Pt atoms ($^1J_{PtH} = 572$ Hz). The spectrum of **3** showed the corresponding peak at $\delta = -5.9$ ppm without any ^{195}Pt satellite peaks. This clearly indicated that the two central M atoms are symmetrically bridged by an acidic hydride, resulting in a MHM three-center two-electron (3c–2e) interaction.

To understand the electronic structure of these complexes, MO calculations were performed for **2** and $[Pt_6(\mu\text{-dpmp})_4(XylNC)_2]^{2+}$ (**C**), a hypothetical hexaplatinum complex that serves as a model contains a Pt^I-$\{Pt^0\}_4$-Pt^I string with the precise CVE of 86.[12] The HOMO of complex **C** lies at high energy and is mainly composed of a p_σ–p_σ bonding interaction of the two central Pt atoms. When a H^+ ion is incorporated between the two central Pt atoms, the HOMO is significantly stabilized due to mixing with the low-lying d_σ–d_σ bonding orbital of the central Pt atoms and the *s* orbital of the H atom, resulting in a somewhat nonbonding character; this factor should be responsible for the stability of the isolated complex **2**.

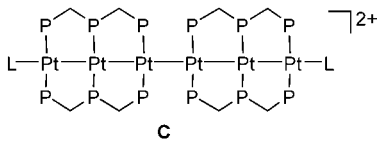

C

In the UV/Vis spectra of complexes **2** and **3**, a very intense and broad absorption was observed around 580 nm (**2**) and 670 nm (**3**), which is characteristic of the MHM 3c–2e interaction. The ESI-TOF mass spectra of **2** and **3** in CH_2Cl_2 showed a trivalent parent peak for $[Pt_4M_2(\mu\text{-H})(\mu\text{-dpmp})_4(XylNC)_2]^{3+}$ at $m/z = 1153.19$ (**2**, M = Pt) and 1094.19 (**3**, M = Pd). These results, along with the $^{31}P\{^1H\}$ NMR spectra (see the Experimental Section), clearly demonstrated that complexes **2** and **3** are stable in solution and exist as linearly ordered hexanuclear molecules.

The cyclic voltammograms of **2** and **3** in CH_3CN showed irreversible multistep oxidation and reduction waves in a potential window of −2.0 to +0.8 V (vs. $Ag/AgPF_6$). Coulometric analyses of complex **2** suggested that the hexametallic core undergoes a two-step, one-electron oxidation at $E_{pa}^1 = -0.16$ V and $E_{pa}^2 = 0.01$ V, a two-electron oxidation at $E_{pa}^3 = 0.41$ V, and one- and two-electron reduction processes at $E_{pc}^1 = -1.23$ V and $E_{pc}^2 = -1.87$ V (Figure 2).[13]

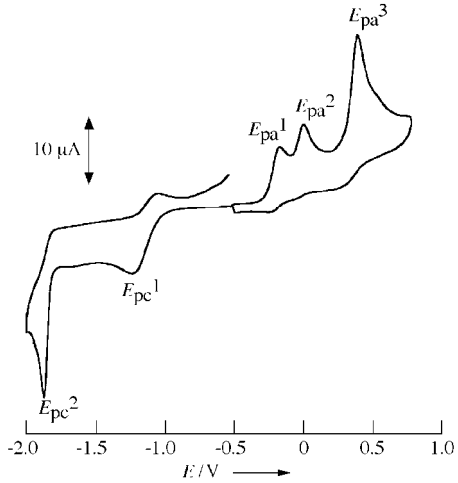

Figure 2. Cyclic voltammogram of **2** in acetonitrile containing 0.1 M (nBu$_4$N)(PF_6) at room temperature with a scan rate of 100 mV s^{-1}. *E* vs. Ag^+/Ag.

The two-electron oxidized hexametallic clusters $[Pt_4M_2(\mu\text{-dpmp})_4(XylNC)_2](PF_6)_4$ (M = Pt (**4**), Pd (**5**)) were isolated by chemical oxidation of **2** and **3** with $[Cp_2Fe][PF_6]$ or HPF_6 as well as by potentiostatic electrolyses (Scheme 1). In the electronic absorption spectra of **4** and **5**, the absorption around 580–670 nm characteristic of the bridging hydride is missing, and the $^{31}P\{^1H\}$ NMR spectra suggested that the linear hexametallic cores remain intact, even in solution.

The structure of **5** was determined by X-ray crystallography (Figure 3).[14] The cluster cation has a charge of +4 with a CVE of 84. Although the $Pt_2Pd_2Pt_2$ hexametallic core is

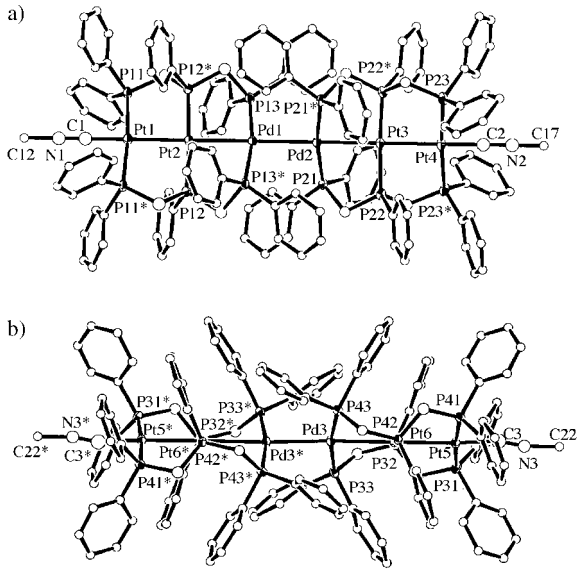

Figure 3. Crystal structure of **5**. The crystal contains two chemically equivalent, independent cluster cations; one cation has a crystallographically imposed C_2 axis along the hexametallic chain (a) and the other cation has a C_2 axis vertical to the metal axis (b). (ORTEP plots; the xylyl rings have been omitted for clarity.) Selected bond distances [Å] and angles [°]: Pt1–Pt2 2.686(1), Pt2–Pd1 2.792(2), Pd1–Pd2 2.844(2), Pt3–Pd2 2.786(2), Pt3–Pt4 2.680(1), Pt5–Pt6 2.6854(9), Pt6–Pd3 2.789(1), Pd3–Pd3* 2.829(3), Pt1–P11 2.301(5), Pt2–P12 2.260(4), Pt3–P22 2.254(5), Pt4–P23 2.300(5), Pt5–P31 2.300(5), Pt5–P41 2.307(5), Pt6–P32 2.244(5), Pt6–P42 2.261(5), Pd1–P13 2.309(5), Pd2–P21 2.314(5), Pd3–P33 2.318(5), Pd3–P43 2.308(5), Pt1–C1 1.86(3), Pt4–C2 1.86(3), Pt5–C3 1.89(2), N1–C1 1.17(3), N2–C2 1.27(3), N3–C3 1.15(2); Pt1-Pt2-Pd1 (= Pt2-Pd1-Pd2 = Pd1-Pd2-Pt3 = Pd2-Pt3-Pt4) 180, Pt5-Pt6-Pd3 179.62(4), Pt6-Pd3-Pd3* 177.93(8), Pt2-Pt1-C1 (= Pt3-Pt4-C2) 180, Pt6-Pt5-C3 176.7(6).

retained, the metal–metal separations are different from those in **3**: $d_{out} = 2.684$ Å (Pt–Pt), $d_{inn} = 2.789$ Å (Pt–Pd), and $d_{cen} = 2.837$ Å (Pd–Pd). The central Pd–Pd distances are decreased by about 0.52 Å and the neighboring Pt–Pd bonds are elongated by about 0.04 Å upon two-electron oxidation or hydride elimination of **3**. The structure indicates the presence of metal–metal bonding between the central M atoms and delocalization of the metal–metal bonding electrons through the inner Pt-Pd-Pd-Pt unit. These results clearly demonstrated that hexametallic strings are redox-active without fragmentation of the cluster core. The bonding electrons in the adjacent M–Pt bonds migrate into the central M–M bond with a redox-coupled dynamic structural change upon two-electron oxidation of the hexametallic string.

In conclusion, the novel hexametallic clusters **2** and **3** were successfully synthesized and were demonstrated to be redox-active. They are readily oxidized to the electron-deficient clusters **4** and **5** with dynamic structural changes to the metal strings. Compounds **2** and **4** can be regarded as rigid-rod, discrete molecules (≈3 nm long) which contain the longest platinum chain known so far.[15] Furthermore, the present methodology could be applied to construct additional long metallic chains in a bottom-up strategy of molecular chemistry, and may lead to the development of molecular-based electronic devices.

Experimental Section

All procedures were performed under a dry nitrogen atmosphere using standard Schlenk techniques.

2: A mixture of **1a**·$(CH_3)_2CO$ (215 mg, 97.2×10^{-3} mmol) and $NaBH_4$ (131 mg, 3.47 mmol) was dissolved in ethanol and stirred for 1 h to generate a brown precipitate. The solvent was removed under reduced pressure, and the brown residue was extracted with CH_2Cl_2. The color of the solution changed from dark green to dark blue within 1 h, and the solution was concentrated. After careful addition of Et_2O, the solution was allowed to stand at 2 °C to afford dark blue cubic crystals of **2**·3 CH_2Cl_2. Yield 88 mg, 44 %; C,H,N analysis (%) calcd for $C_{149}H_{141}Cl_6F_{18}N_2P_{15}Pt_6$: C 43.13, H 3.42, N 0.68; found: C 42.92, H 3.45, N 0.64; IR (KBr): $\tilde{\nu} = 2131$ (N≡C), 839 cm^{-1} (PF_6); UV/Vis (CH_2Cl_2): λ_{max} (ε) = 583 (9.63×10^4), 402 (3.14×10^4), 379 nm (2.74×10^4); ^{1}H NMR (300 MHz, CD_2Cl_2, RT): $\delta = 8.7$–6.2 (m, 106H, Ar), 5.1–4.7 (m, 8H, CH_2), 2.6 (br m, 4H, CH_2), 1.8 (br m, 4H, CH_2), 1.24 (s, 12H, *o*-CH_3), −8.61 ppm (br m, 1H, Pt–H, $^1J_{PtH} = 572$ Hz); $^{31}P\{^1H\}$ NMR (121 MHz, CD_2Cl_2, RT): $\delta = 6.5$ (m, 4P, $^1J_{PtP} = 3395$ Hz), −3.0 (m, 4P, $^1J_{PtP} = 2938$ Hz), −15.3 ppm (m, 4P, $^1J_{PtP} = 3002$ Hz); ESI-MS (CH_2Cl_2): *m*/*z* (*z*): 1153.194 (3) $[Pt_6(H)(dpmp)_4(XylNC)_2]^{3+}$ (1153.179).

3: Complex **1b**·$(CH_3)_2CO$ (189 mg, 89.2×10^{-3} mmol) and NaOMe (97 mg, 1.79 mmol) were dissolved in CH_2Cl_2/MeOH (1/1), and the mixture was stirred overnight. The color of the solution changed from orange to dark blue-green. The solvent was removed under reduced pressure, and the residue was extracted with CH_2Cl_2. The extract was concentrated, and careful addition of Et_2O afforded dark blue-green cubic crystals of **3**. Yield 84 mg, 51 %; C,H,N analysis (%) calcd for $C_{146}H_{135}F_{18}N_2P_{15}Pd_2Pt_4$: C 47.17, H 3.66, N 0.75; found: C 46.97, H 3.65, N 0.81; IR (KBr): $\tilde{\nu} = 2135$ (N≡C), 841 cm^{-1} (PF_6); UV/Vis (CH_2Cl_2): λ_{max} (ε) = 674 (8.48×10^4), 438 (1.02×10^4), 395 (1.77×10^4), 346 nm (2.00×10^4); ^{1}H NMR (300 MHz, CD_2Cl_2, RT): $\delta = 8.7$–6.2 (m, 106H, Ar), 5.2–4.3 (m, 8H, CH_2), 2.7 (br m, 4H, CH_2), 1.9 (br m, 4H, CH_2), 1.23 (s, 12H, *o*-CH_3), −5.90 ppm (m, 1H, Pd–H); $^{31}P\{^1H\}$ NMR (121 MHz, CD_2Cl_2, RT): $\delta = 3.3$ (m, 4P), −3.3 (m, 4P, $^1J_{PtP} = 2938$ Hz), −11.0 ppm (m, 4P, $^1J_{PtP} = 2948$ Hz); ESI-MS (CH_2Cl_2): *m*/*z* (*z*): 1094.194 (3) $[Pt_4Pd_2(H)(dpmp)_4(XylNC)_2]^{3+}$ (1094.139).

4: $[Cp_2Fe](PF_6)$ (5.7 mg, 17×10^{-3} mmol) was added to a solution of **2**·3 CH_2Cl_2 (35 mg, 8.4×10^{-3} mmol) in CH_2Cl_2, and the solution was stirred for 2 h. The solvent was removed under reduced pressure, and the black residue was washed with Et_2O and extracted with CH_2Cl_2. The extract was concentrated and addition of Et_2O afforded dark-green crystals of **4**·3.5 CH_2Cl_2. Yield 18 mg, 49 %; C,H,N analysis (%) calcd for $C_{149.5}H_{141}Cl_7F_{24}N_2P_{16}Pt_6$: C 41.41, H 3.28, N 0.65; found: C 41.27, H 3.07, N 0.91; IR (KBr): $\tilde{\nu} = 2161$ (N≡C), 840 cm^{-1} (PF_6); UV/Vis (CH_2Cl_2): λ_{max} (ε) = 420 (2.16×10^4), 377 (7.11×10^4), 310 (sh, 4.06×10^4), 289 nm (sh, 5.06×10^4); ^{1}H NMR (300 MHz, [D_6]acetone, RT): $\delta = 8.3$–6.7 (m, 106H, Ar), 5.0 (m, 8H, CH_2), 4.3 (br m, 4H, CH_2), 3.6 (br m, 4H, CH_2), 1.57 ppm (s, 12H, *o*-CH_3); $^{31}P\{^1H\}$ NMR (121 MHz, [D_6]acetone, RT): $\delta = 20.8$ (m, 4P, $^1J_{PtP} = 3413$ Hz), −1.1 (m, 4P, $^1J_{PtP} = 2741$ Hz), −6.9 ppm (m, 4P, $^1J_{PtP} = 2797$ Hz).

5: A similar procedure to that for complex **4** using **3** as the starting material gave **5**·CH_2Cl_2. Yield 24 mg, 54 %; C,H,N analysis (%) calcd for $C_{147}H_{136}N_2P_{16}F_{24}Cl_2Pt_4Pd_2$: C 44.74, H 3.47, N 0.71; found: C 44.27, H 3.86, N 0.71; IR (KBr): $\tilde{\nu} = 2162$ (N≡C), 839 cm^{-1} (PF_6); UV/Vis (CH_2Cl_2): λ_{max} (ε) = 461 (3.45×10^4), 370 (7.51×10^4), 343 (5.55×10^4), 310 nm (sh, 5.08×10^4); ^{1}H NMR (300 MHz, CD_3CN, RT): $\delta = 8.0$–6.8 (m, 106H, Ar), 4.7 (m, 8H, CH_2), 4.1 (br m, 4H, CH_2), 3.8 (br m, 4H,

CH_2), 1.48 ppm (s, 12H, *o*-CH_3); $^{31}P\{^1H\}$ NMR (121 MHz, CD_3CN, RT): $\delta = 5.9$ (m, 4P), 0.4 (m, 4P, $^1J_{PtP} = 2766$ Hz), −11.1 ppm (m, 4P, $^1J_{PtP} = 2887$ Hz).

Received: May 18, 2004

Keywords: cluster compounds · oxidation · palladium · platinum · redox chemistry

[1] a) *Metal–Metal Bonds and Clusters in Chemistry and Catalysis* (Ed.: J. P. Fackler), Plenum, New York, **1990**; b) D. A. Adams, F. A. Cotton, *Catalysis by Di- and Polynuclear Metal Cluster Complexes,* Wiley, New York, **1998**.

[2] a) S.-Y. Lai, T.-W. Lin, Y.-H. Chen, C.-C. Wang, G.-H. Lee, M.-H. Yang, M.-K. Leung, S.-M. Peng, *J. Am. Chem. Soc.* **1999**, *121*, 250; b) Y.-H. Chen, C.-C. Lee, C.-C. Wang, G.-H. Lee, S.-Y. Lai, F.-Y. Li, C.-Y. Mou, S.-M. Peng, *Chem. Commun.* **1999**, 1667; c) C.-C. Wang, W.-C. Lo, C.-C. Chou, G.-H. Lee, J.-M. Chen, S.-M. Peng, *Inorg. Chem.* **1998**, *37*, 4059; d) S.-J. Shieh, C.-C. Chou, G.-H. Lee, C.-C. Wang, S.-M. Peng, *Angew. Chem.* **1997**, *109*, 57; *Angew. Chem. Int. Ed. Engl.* **1997**, *36*, 56.

[3] a) R. Clérac, F. A. Cotton, K. R. Dunbar, T. Lu, C. A. Murillo, X. Wang, *J. Am. Chem. Soc.* **2000**, *122*, 2272; b) F. A. Cotton, L. M. Daniels, C. A. Murillo, X. Wang, *Chem. Commun.* **1999**, 2461.

[4] a) T. Murahashi, T. Uemura, H. Kurosawa, *J. Am. Chem. Soc.* **2003**, *125*, 8436; b) T. Murahashi, Y. Higuchi, T. Katoh, H. Kurosawa, *J. Am. Chem. Soc.* **2002**, *124*, 14288; c) T. Murahashi, T. Nagai, T. Okuno, T. Matsutani, H. Kurosawa, *Chem. Commun.* **2000**, 1689; d) T. Murahashi, E. Mochizuki, Y. Kai, H. Kurosawa, *J. Am. Chem. Soc.* **1999**, *121*, 10660.

[5] a) K. Mashima, H. Nakano, A. Nakamura, *J. Am. Chem. Soc.* **1996**, *118*, 9083; b) K. Mashima, M. Tanaka, K. Tani, A. Nakamura, S. Takeda, W. Mori, K. Yamaguchi, *J. Am. Chem. Soc.* **1997**, *119*, 4307; c) K. Mashima, A. Fukumoto, H. Nakano, Y. Kaneda, K. Tani, A. Nakamura, *J. Am. Chem. Soc.* **1998**, *120*, 12151.

[6] C. Tejel, M. A. Ciriano, B. E. Villarroya, J. A. López, F. J. Lahoz, L. A. Oro, *Angew. Chem.* **2003**, *115*, 547; *Angew. Chem. Int. Ed.* **2003**, *42*, 530.

[7] T. Zhang, M. Drouin, P. D. Harvey, *Inorg. Chem.* **1999**, *38*, 957.

[8] a) T. Tanase, H. Ukaji, T. Igoshi, Y. Yamamoto, *Inorg. Chem.* **1996**, *35*, 4114; b) T. Tanase, H. Toda, Y. Yamamoto, *Inorg. Chem.* **1997**, *36*, 1571; c) T. Tanase, H. Ukaji, H. Takahata, H. Toda, T. Igoshi, Y. Yamamoto, *Organometallics* **1998**, *17*, 196; d) T. Tanase, R. A. Begum, *Organometallics* **2001**, *20*, 106; e) T. Tanase, R. A. Begum, H. Toda, Y. Yamamoto, *Organometallics* **2001**, *20*, 968.

[9] Although the mechanism of formation for **3** was not clear and no intermediate species were monitored, experiments with ^2H-labeled solvents suggested that the hydride H atom was derived from C–H cleavage of methanol or methoxide.

[10] Crystal data for **2**·4 CH_2Cl_2·3 H_2O ($C_{150}H_{148}Cl_8F_{18}N_2P_{15}Pt_6O_3$): $M_r = 4287.57$ ($0.25 \times 0.25 \times 0.20$ mm), triclinic, space group $P\bar{1}$ (no. 2), $a = 20.6075(9)$, $b = 21.874(1)$, $c = 18.1441(8)$ Å, $\alpha = 91.065(3)$, $\beta = 89.810(3)$, $\gamma = 94.661(3)°$, $V = 8150.4(6)$ Å^3, $Z = 2$, $\rho_{calcd} = 1.747$ g cm^{-3}, $F(000) = 4154$, $2\theta_{max} = 52°$, $Mo_{K\alpha}$ radiation ($\lambda = 0.71070$ Å, $\mu = 54.58$ cm^{-1}), $T = -120$ °C. A total of 27996 reflections were collected with a Rigaku/MSC Mercury CCD diffractometer ($2\theta = 6$–$55°$, ω scans 0.25°). The crystal structure was solved by direct methods (SIR98) and refined with full-matrix least-squares techniques (teXsan). Non-hydrogen atoms were anisotropically refined, expect for some atoms of the solvent molecules. The bridging H atom was not located, and the positions of carbon-bound H atoms were calculated and not refined. Final $R_1 = 0.054$ and $R_w = 0.067$ (19103 reflections, $I > 2\sigma(I)$, $6 < 2\theta < 52°$) for 1811 variables. CCDC-238886 (**2**), CCDC-238887 (**3**), and CCDC-238888 (**5**) contain the supplementary crystallographic data for this paper. These data can be obtained free of charge via www.ccdc.cam.ac.uk/conts/retrieving.html (or from the Cambridge Crystallographic Data Centre, 12, Union Road, Cambridge CB21EZ, UK; fax: (+44)1223-336-033; or deposit@ccdc.ca.ac.uk). The ORTEP plot for complex **3** is available in the Supporting Information.

[11] Crystal data for **3**·5 CH_2Cl_2·CH_3OH·4 H_2O ($C_{152}H_{156}Cl_{10}F_{18}N_2P_{15}Pd_2Pt_4O_5$): $M_r = 4245.18$ ($0.30 \times 0.25 \times 0.10$ mm), triclinic, space group $P\bar{1}$ (no. 2), $a = 18.290(1)$, $b = 20.7102(5)$, $c = 22.070(2)$ Å, $\alpha = 94.231(5)$, $\beta = 90.730(1)$, $\gamma = 90.1903(8)°$, $V = 8336.3(10)$ Å^3, $Z = 2$, $\rho_{calcd} = 1.691$ g cm^{-3}, $F(000) = 4166$, $2\theta_{max} = 54.7°$, $Mo_{K\alpha}$ radiation ($\lambda = 0.71070$ Å, $\mu = 39.17$ cm^{-1}), $T = -120$ °C. Data were collected with a Rigaku/MSC Mercury CCD diffractometer ($2\theta = 6$–$52°$, ω scans 0.25°). The crystal structure was solved by Patterson methods (Dirdif94 Patty) and refined with teXsan. Non-hydrogen atoms were anisotropically refined, except for some atoms of the solvent molecules. The bridging H atom was not located, and the positions of carbon-bound H atoms were calculated and not refined. Final $R_1 = 0.064$ and $R_w = 0.081$ for 1769 variables (18753 reflections, $I > 3\sigma(I)$, $6 < 2\theta < 52°$).

[12] The EHMO calculations were carried out on the model compound for **2**, and a simplified fragment MO interaction diagram is provided in the Supporting Information. Single point density functional calculations on the crystal structure of the complex cation of **2** were also carried out by the BECK3LYP method with the LANL2DZ basis set with the program Gaussian 98.

[13] Cyclic voltammograms were measured with the following electrodes: glassy carbon (working), Pt coil (counter), Ag/$AgPF_6$ (reference). The cyclic voltammogram of **3** was similar to that of **2**, except that the first two-step oxidation waves at $E_{pa}{}^1 = -0.16$ V and $E_{pa}{}^2 = 0.01$ V in complex **2** were observed as a broad, one-step oxidation wave at $E_{pa}{}^1 = -0.21$ V. Under the experimental conditions, the ferrocene/ferrocenium redox couple was observed at 0.09 V.

[14] Crystal data for **5**·7 CH_2Cl_2 ($C_{153}H_{148}Cl_{14}F_{24}N_2P_{16}Pd_2Pt_4$): $M_r = 4455.91$ ($0.35 \times 0.30 \times 0.28$ mm), orthorhombic, space group $C222_1$ (no. 20), $a = 26.4070(9)$, $b = 40.588(1)$, $c = 41.353(1)$ Å, $V = 44322(2)$ Å^3, $Z = 8$, $\rho_{calcd} = 1.335$ g cm^{-3}, $F(000) = 17424$, $2\theta_{max} = 55.0°$, $Mo_{K\alpha}$ radiation ($\lambda = 0.71070$ Å, $\mu = 30.06$ cm^{-1}), $T = -120$ °C. Data were collected with Rigaku/MSC Mercury CCD diffractometer ($2\theta = 6$–$55°$, ω scans 0.25°). The crystal structure was solved by Patterson methods (DIRDIF94 Patty) and refined with teXsan. The crystal contains two chemically equivalent, independent cluster cations; one cation (Figure 3a) has a crystallographically imposed C_2 axis along the hexametallic chain and the other cation (Figure 3b) has a C_2 axis vertical to the metal axis. The Pt, Pd, P, and F atoms were refined with anisotropic thermal parameters, and other non-hydrogen atoms were refined. Hydrogen atoms were calculated and not refined. Final $R_1 = 0.069$ and $R_w = 0.086$ for 1087 variables (15979 reflections, $I > 3\sigma(I)$, $6 < 2\theta < 55°$).

[15] Molecular compounds containing low-valent Pt chains are rare. The linear tetraplatinum complex reported in ref. [7] was the longest molecule thus far. In contrast, linearly assembled high-valent Pt compounds in the solid state have been well studied. See, for example, a) K. Matsumoto, K. Sakai, *Adv. Inorg. Chem.* **2000**, *49*, 375; b) K. Matsumoto, K. Sakai, K. Nishio, Y. Tokisue, R. Ito, T. Nishide, Y. Shichi, *J. Am. Chem. Soc.* **1992**, *114*, 8110.

